Proceedings of the 21st ICSMGE, Vienna, Austria, 14 – 19 June 2026. Pistrol, Adam & Schweiger (eds.)
Published by: ÖGG, Austrian Society for Geomechanics, Salzburg, Austria, ISBN 978-3-9503898-4-5
https://doi.org/10.53243/ICSMGE2026-934

A Critical Appraisal of Weak Rock *P-y* Models for Laterally Loaded Piles in Chalk

Zijing Xu, Andrea Diambra, Tingfa Liu, Borui Ge
School of Civil, Aerospace and Design Engineering, University of Bristol, Bristol, UK, au24264@bristol.ac.uk

ABSTRACT: The *P-y* method is probably the most extensively used tool in practical design of laterally loaded piles. Most traditional *P-y* models were primarily developed for clays and sands and are unsuitable for direct application for weak rocks, such as chalk, due to significant differences in materials' physical properties and mechanical behaviour. This paper presents a critical appraisal of available *P-y* models specifically developed for weak rocks and chalk with the aim to identify the most suitable and accurate models for predicting lateral pile behaviour in such geomaterials. Key features of the selected *P-y* models are summarised, and their suitability and performance are assessed by comparing model predictions with measurements from field pile tests in chalk that cover a range of pile geometries. Steps are then presented for adjusting some of the model parameters to better capture the lateral loading response over small and large displacement ranges. The results demonstrate that the McAdam et al. (2024) model shows the best overall accuracy and consistency, and the performance of the Reese (1997) model can be improved substantially by re-calibrating the strength reduction factor. Specific recommendations are provided for selecting and optimising *P-y* models tailored for chalk and other weak rock formations.

KEYWORDS: Laterally Loaded Piles, *P-y* Models, Weak Rocks, Pile Behaviour, Model Evaluation.

1 INTRODUCTION

The design of laterally loaded piles commonly relies on a simplified one-dimensional analysis framework known as the *P-y* method (with *P* signifying lateral force per unit depth and *y* lateral displacement). The *P-y* method is developed based on the Winkler (1867) beam theory in which the ground is modelled as a series of independent non-linear springs along the embedded pile length.

A wide range of *P-y* models have been developed primarily for piles in sands and clays, alongside other specific loading conditions such as cyclic or multi-directional loading. Recent advancements have also been made for large diameter laterally loaded monopiles. New *P-y* formulations, procedures for their derivations and the account of additional soil resistance components were proposed for example in the PISA project (Burd et al., 2020; Byrne et al., 2020).

In contrast, there has been relatively limited consideration of *P-y* curves for piles in weak and hard rocks which are becoming increasingly common as offshore wind developments expand into new areas, particularly across Northwestern Europe and in the North, Baltic and Celtic Seas.

Previous *P-y* models for rock include those proposed by Fragio et al. (1985) and Reese (1997). Erbrich (2004) proposed the CHIPPER model, which accounts for progressive rock breakage (chipping) induced by lateral loading. Based on field pile tests from the Wind Support project (Ciavaglia et al., 2017), Muir Wood et al. (2015) proposed a framework of bi-linear *P-y* curves for piles in chalk. More recently, McAdam et al. (2024) proposed a specific *P-y* model for chalk based on a more extensive pile testing programme at the same chalk site as part of the ALPACA joint industry project (JIP).

The above-mentioned models have their own distinct features, leading to significant differences and uncertainties when making design choices. Therefore, this study aims to evaluate the broader applicability of selected *P-y* formulations developed for weak rocks and to investigate their key differences. The assessment is carried out by benchmarking the performance of different formulations against laterally loaded pile tests in chalk conducted as part of the Wind Support and the ALPACA projects. The goal is to provide critical review of the applicability of historical *P-y* models and to offer potential suggestions for improving their performance and accuracy for predicting driven piles in chalk and potentially other weak rock conditions.

2 ANALYSED *P-Y* FORMULATIONS FOR ROCKS

A key distinction among *P-y* formulations for weak rocks lies in whether the potential of brittle failure near the rock surface is considered. Assumed failure mechanisms in these formulations typically fall into two categories: ductile and brittle. Some researchers argue that brittle formulations better reflect the abrupt failure mechanisms observed in rock mass, while others suggest that ductile formulations fit observed responses more accurately (Reese, 1997; Erbrich, 2004). Correspondingly, the mathematical forms for *P-y* curves often include power, hyperbolic, or hyperbolic tangent functions. These expressions generally approach an asymptotic value defined as the ultimate force per unit length P_u, or equivalently, ultimate pressure per unit area $p_u = P_\mathrm{u}/D$. Three typical *P-y* formulations developed for weak rocks are selected in this study as summarised in Table 1.

Table 1. Summary of the selected *P-y* formulations

P-y model	Rock type	Failure mode	Tests
Fragio et al. (1985)	Calcareous Claystone	Brittle near the surface and ductile deeper	Bored piles, D=0.405 m
Reese (1997)	Limestone/ Sandstone	Ductile	Bored piles, L/D=6 to 11
McAdam et al. (2024)	Chalk	Ductile	Driven piles, L/D=6, 20

2.1 *Fragio et al. (1985) model*

Fragio et al. (1985) considered calcareous claystone and proposed a *P-y* relationship incorporating both intact peak resistance and residual strength, as shown in Figure 1. The model considers the ultimate lateral resistance P_u increases linearly with depth, starting from $P_\mathrm{u} = 3S_uD$ at ground surface and reaching a maximum $P_\mathrm{u} = 9S_uD$ at depths exceeding 6D, where S_u denotes rock mass shear strength and D pile diameter. The difficulty in applying this model lies in selecting appropriate parameters, particularly because effective shear strength of rock mass may be as low as 10% of the intact unconfined compressive strength for naturally jointed but relatively strong rocks.

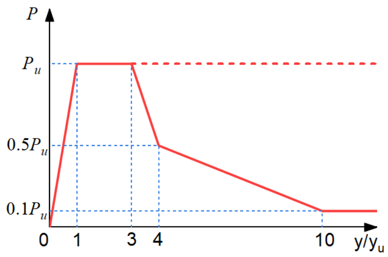

Figure 1. *P-y* curve for claystone (Fragio et al., 1985)

2.2 *Reese (1997) model*

In contrast, Reese (1997) developed a ductile model for bored piles in intermediate rocks such as limestone and sandstone, incorporating the concept of strength degradation. The shape of the *P-y* curve is illustrated in Figure 2. Reese (1997) adopted a simple linear variation of the ultimate resistance, with P_{u} varying as:

$$P_{\mathrm{u}} = \alpha_r\, q_{UCS} D \left[1 + 1.4\left(\frac{z}{D}\right)\right] \leq 5.2\alpha_r q_{UCS} D \tag{1}$$

where q_{UCS} signifies rock's unconfined compression strength, α_r is strength reduction factor.

Reese (1997) incorporated the concept of strength degradation and employed the adjustment parameter α_r to account for strength degradation of weak rock. It varies from 0.33 for RQD = 100% (maximum strength loss) to 1.0 for RQD = 0 (no further loss).

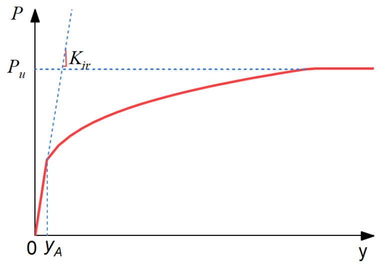

Figure 2. *P-y* curve for weak rock (Reese, 1997)

2.3 *McAdam et al. (2024) model*

More recently, a depth-independent ductile soil reaction curve for chalk was developed by McAdam et al. (2024) based on the field pile tests of the ALPACA project. The curve characterises the relationship between the distributed lateral soil reaction p and the corresponding lateral displacement y. The formulation is expressed as:

$$-n\left(\frac{p}{p_u} - \frac{y}{y_u}\right)^2 + (1-n)\left(\frac{p}{p_u} - \frac{yk_p}{p_u}\right)\left(\frac{p}{p_u} - 1\right) = 0 \tag{2}$$

where p_u is ultimate soil pressure, k_p is initial subgrade modulus, y_u is ultimate displacement, n is a curvature parameter.

Since the other two models describe the relationship between the soil resistance P and the lateral displacement y, the soil pressure p in the McAdam et al. (2024) model needs to be converted to soil resistance P with $P = pD$. The resulting *P-y* curve derived from this formulation is presented in Figure 3. The McAdam et al. (2024) model demonstrated good performance when applied to the Wind Support and ALPACA lateral pile tests. It is important to note that the model parameters and constants were derived through least-squares curve fitting without direct connection with rock properties. Consequently, the applicability of the McAdam et al. (2024) model may be limited to conditions similar to those represented by the pile test cases, and caution should be exercised when extending the model to other rock types or geological settings. Further studies by finite element analysis have investigated the connections between lateral resistance and chalk's stiffness and strength parameters, with detailed considerations of installation effects and fracturing of surrounding chalk mass, local brittleness and stiffness nonlinearity and pressure dependency (Pedone et al., 2023; Kontoe et al., 2025).

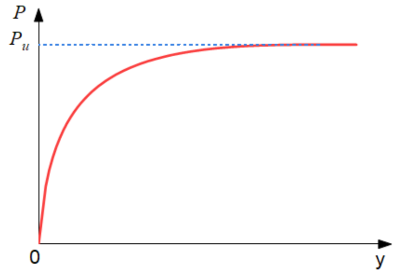

Figure 3. *P-y* curve for chalk (McAdam et al., 2024)

3 MODEL PERFORMANCE EVALUATION

3.1 *Field test cases*

A series of lateral load tests on steel driven piles in low-to medium-density chalk was performed in Kent, UK, as part of the Wind Support and ALPACA joint industry projects. Site investigation campaigns reported an average unconfined compressive strength (UCS) of ≈2.4 MPa (Ciavaglia et al., 2017). The average equivalent Tresca shear strength (S_u) was adopted as 1.32 MPa from Vinck et al. (2024). The Rock Quality Designation (RQD) values exhibited variations with depth with an average of ≈45%.

Three piles of different diameters and L/D ratios were analysed: LD11, TP2 and Pile 3. Piles LD11 and TP2 were from the ALPACA project. LD11 was a 0.508 m outer diameter open steel pile embedded to a depth of 10.16 m, while TP2 had larger outer diameter of 1.22 m but shorter length of 7.32 m. Pile 3 was from the Wind Support project with an outer diameter of 0.762 m and embedded length of 4 m. Field test data of the LD11 case were used to calibrate model parameters, while TP2 and Pile 3 were adopted as validation cases. All these cases were examined in the numerical study by Kontoe et al. (2025) with explicit consideration and modelling of installation effects, which offered a useful reference for the calibration and modification of the *P-y* models, as discussed later.

3.2 *Assessment metric*

Two indices, accuracy metric η and ratio metric ρ, were introduced to enable quantification of model performance across the pile cases, following Burd et al. (2020):

$$\eta = \frac{A_{\mathrm{ref}} - A_{\mathrm{diff}}}{A_{\mathrm{ref}}} \tag{3}$$

where A_{ref} is the reference area typically determined from experimental measurements, A_{diff} represents the deviation area between the 1D model prediction and the reference curve.

$$\rho = \frac{H_{\mathrm{1D}}}{H_{\mathrm{Field}}} \tag{4}$$

where H_{Field} refers to lateral force measured from field test at a specific ground level displacement v_{G}, while H_{1D} represents predicted lateral force at the equivalent displacement.

3.3 *Calibration*

Analysis was firstly conducted for pile LD11 to calibrate the *P-y* model inputs. The shear strength input in the Fragio et al. (1985) model was taken as laboratory measurements on intact specimens, while the Reese (1997) model requires more complex inputs, as listed in Table 2. The McAdam et al. (2024) model kept the initially proposed input values.

Field lateral load-displacement data of pile LD11 were compared with the predictions by Reese (1997), Fragio et al. (1985) and McAdam et al. (2024) models, as shown in Figure 4. It is observed that Reese (1997) model significantly overpredicts the ultimate lateral resistance. This discrepancy is likely due to that pile LD11 was driven rather than drilled and grouted, resulting in de-structuration and additional fracturing in the chalk surrounding the pile. Reese (1997) assumed that fracturing occurs at the rock surface under small deflections and introduces a factor α_r to account for this effect. In addition, due to pile installation effects, a reduction factor of 0.35 was applied. Considering both influences on compressive strength, α_r is adjusted to 0.245. The input parameters and calibration factors used in the Reese (1997) model are summarised in Table 2. Compared to Reese (1997), the Fragio et al. (1985) curve exhibits significantly lower initial stiffnesses that are closer to the field test results. However, the model assumes an initial linear response and the discrepancies between predictions and field tests increase at greater displacements. The McAdam et al. (2024) model demonstrated the best overall performance against the field measurements.

Table 2. Reese (1997) input parameters

Parameter	Symbol	Unit	Value	Calibration
Displacement parameter	k_{rm}	-	0.0005	0.0005
Initial reaction modulus	E_{ir}	GPa	4	4
Strength reduction factor	α_r	-	0.7	0.245
Compressive strength	q_{UCS}	MPa	2.4	2.4

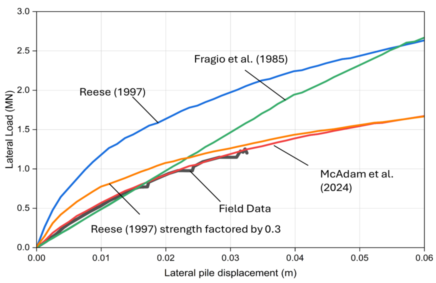

Figure 4. Assessment of method performance against pile LD11

3.4 *Model performance assessment*

To validate the effectiveness of the calibration, the same set of input parameters was used to predict the responses of the other two test cases of Pile 3 and TP2, as plotted in Figures 5 and 6. It can be observed that the load–displacement curves predicted by McAdam et al. (2024) model match well with the field data for both piles. The calibrated Reese (1997) model also produces relatively close match with the measured data with modest underestimation in ultimate capacities. In contrast, the Fragio et al. (1985) model predictions deviate significantly from the field measurements.

Comparisons of the performance of the various models in predicting the lateral response of different piles were conducted using the accuracy and capacity ratio metrics defined in Equations (3) and (4) over large and small displacement ranges. If the measured curves did not reach the ultimate state, a cubic spline was used to extrapolate the backbone curves to D/10. The results are summarised in Table 3 and Table 4, where the η and ρ metrics were evaluated over the displacement ranges of $0 < v_G < D/10$ and $0 < v_G < D/10000$, respectively.

Table 3. *P-y* model performance assessment over large displacement range ($0 < v_G < D/10$)

P-y model	LD11 (L/D=20)		Pile 3 (L/D=5)		TP2 (L/D=6)	
	η	ρ	η	ρ	η	ρ
Fragio et al. (1985)	0.73	1.53	0.41	2.11	0.42	1.97
Reese (1997)	0.90	1.02	0.81	0.86	0.87	0.86
McAdam et al. (2024)	0.99	1.02	0.97	0.99	0.98	1.01

Table 4. *P-y* model performance assessment over small displacement range ($0 < v_G < D/10000$)

P-y model	LD11 (L/D=20)		Pile 3 (L/D=5)		TP2 (L/D=6)	
	η	ρ	η	ρ	η	ρ
Fragio et al. (1985)	0.44	0.44	-0.64	2.61	0.23	0.23
Reese (1997)	0.85	1.16	-8.33	10.32	0.50	0.50
McAdam et al. (2024)	0.73	0.74	-2.54	4.44	0.42	0.43

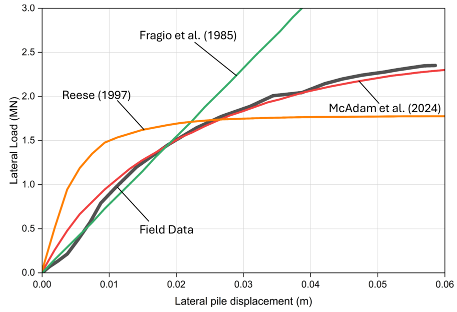

Figure 5. Measured and computed responses for Pile 3

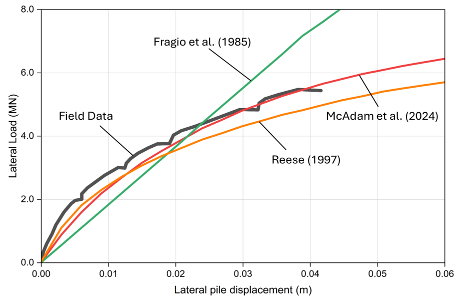

Figure 6. Measured and computed responses for TP2

Table 3 summarises the accuracy and capacity ratio metrics at ultimate limit state. Among the three methods, Fragio et al. (1985) showed the lowest prediction accuracy, with η values ranging from 0.41 to 0.73 and consistently overestimating the ultimate capacity by an average of 87%. Reese (1997) model yielded good performance for the long pile LD11 with η = 0.90 and ρ = 1.02, but the prediction accuracy remained relatively low for the shorter piles (Pile 3 and TP2). In contrast, McAdam et al. (2024) model demonstrated high and consistent accuracy across all the three piles analysed, with accuracy metrics ranging from 0.97 to 0.99 and ratio metrics between 0.99 and 1.02, indicating close agreements with the field measurements.

Moving onto small displacement response, as listed in Table 4, all methods exhibited significant deviations from the measured data, particularly for the short Pile 3. This is primarily due to the convex shape of the initial part of the load–displacement curve caused by remoulded chalk annuli generated post-installation and progressive closure of fractures during lateral loading (Ciavaglia et al., 2017). The accuracy ratios of all three *P-y* models remained relatively low for the pile cases analysed, reflecting the limitations of the existing *P-y* models in capturing pile response over small displacements in chalk.

Overall, the McAdam et al. (2024) model is shown to produce best fit to field pile experiments in chalk. The model assumes a constant ultimate lateral resistance with depth, which is appropriate for cases where the ultimate resistance is not directly positively correlated with depth. The model employs a single best-fit soil reaction curve. Although local deviations may exist between the fitted curve and actual soil responses, integrating the soil reactions along the pile length appears to average out these discrepancies, leading to overall accurate predictions of global load-displacement response. These characteristics make the model well-conditioned and effective for capturing lateral pile response in chalk.

4 CONCLUSIONS

This study assessed the performance of three existing *P-y* models, Fragio et al. (1985), Reese (1997) and McAdam et al. (2024), for predicting lateral loading response of driven piles in chalk for selected Wind Support and ALPACA test cases. Model performance was assessed quantitatively by accuracy and ratio metrics over ultimate and small displacement ranges. Among the three models, the McAdam et al. (2024) model showed the best consistent and accurate predictions across different pile geometries. The Fragio et al. (1985) model tended to provide non-conservative estimates of ultimate capacities but underestimated stiffnesses at small displacements. The performance of the Reese (1997) model appears to be dependent on pile length-to-diameter (L/D) ratio. By calibrating the model using the LD11 field data and applying a strength reduction factor of 0.35, the load–displacement predictions improved significantly for this specific case. Similar improvement, however, was not seen in other pile cases. All three models appeared to capture the small displacement stiffness relatively poorly.

Driven pile installation causes additional fracturing in chalk and further strength reductions from the in-situ state. The strength reduction factor introduced in the Reese (1997) model provides an effective means to account for strength degradation and link to measurable rock quality index. Future work will focus on how to systematically adjust the strength reduction factor α_r and examine the influence of varying L/D ratios on model performance for a range of weak rocks beyond chalk.

5 ACKNOWLEDGEMENTS

The first author is grateful for the financial support provided by the University of Bristol and China Scholarship Council (CSC).

6 REFERENCES

Burd, H. J., Taborda, D. M., Zdravković, L., Abadie, C. N., Byrne, B. W., Houlsby, G. T., Gavin, K. G., Igoe, D. J., Jardine, R. J., Martin, C. M., & others. (2020). PISA design model for monopiles for offshore wind turbines: Application to a marine sand. *Géotechnique*, *70*(11), 1048–1066.

Byrne, B. W., Houlsby, G. T., Burd, H. J., Gavin, K. G., Igoe, D. J., Jardine, R. J., Martin, C. M., McAdam, R. A., Potts, D. M., Taborda, D. M., & others. (2020). PISA design model for monopiles for offshore wind turbines: Application to a stiff glacial clay till. *Géotechnique*, *70*(11), 1030–1047.

Ciavaglia, F., Carey, J. and Diambra, A., 2017. Monotonic and cyclic lateral tests on driven piles in Chalk. Proceedings of the Institution of Civil Engineers-Geotechnical Engineering, 170(4), pp.353–366.

Erbrich, C.T., 2004. A New Method for the Design of Laterally Loaded Anchor Piles in Soft Rock. In: Offshore Technology Conference. [online] Offshore Technology Conference. Houston, Texas: OTC. https://doi.org/10.4043/16441-ms.

Fragio, A., Santiago, J. and Sutton, V., 1985. Load tests on grouted piles in rock. In: Offshore Technology Conference. OTC. p.OTC-4851.

Muir Wood, A., Mackenzie, B., Burbury, D., Rattley, M., Clayton, C., Mygind, M., Andersen, K.W., Thilsted, C.L. and Liingaard, M.A., 2015. Design of large diameter monopiles in chalk at Westermost Rough offshore wind farm. In: Frontiers in Offshore Geotechnics III: Proceedings of the 3rd International Symposium on Frontiers in Offshore Geotechnics (ISFOG 2015). Taylor & Francis Books Ltd. pp.723–728.

McAdam, R.A., Buckley, R.M., Schranz, F., Byrne, B.W., Jardine, R.J., Kontoe, S., Liu, T., Vinck, K. and Crispin, J.J., 2024. Monotonic and cyclic lateral loading of piles in low- to medium-density chalk. Géotechnique, pp.1 – 17. https://doi.org/10.1680/jgeot.23.00484.

Reese, L.C., 1997. Analysis of Laterally Loaded Piles in Weak Rock. J. Geotech. Geoenviron. Eng., 123(11), pp.1010–1017.https://doi.org/10.1061/(asce)10900241(1997)123:11(1010).

Kontoe, S., Bellumat, E., Pedone, G. and Jardine, R., 2025. 3D FE analysis of laterally loaded piles driven in chalk. In: 5th international symposium on frontiers in offshore geotechnics. Nantes, France. https://doi.org/10.53243/ISFOG2025-608.

Pedone, G., Kontoe, S., Zdravković, L., Jardine, R.J., Vinck, K. and Liu, T., 2023. Numerical modelling of laterally loaded piles driven in low-to-medium density fractured chalk. Computers and Geotechnics, 156, p.105252.

Vinck, K., Ahmadi-Naghadeh, R., Buckley, R.M., Byrne, B.W., Lawrence, J.A., Mcadam, R.A. and Schranz, F., 2024. Advanced in situ and laboratory characterisation of the ALPACA chalk research site. Géotechnique, 74(6), pp.512–526. https://doi.org/10.1680/jgeot.21.00197.

Winkler, E., 1867. Die Lehre von der Elasticitaet und Festigkeit: mit besonderer Rücksicht auf ihre Anwendung in der Technik, für polytechnische Schulen, Bauakademien, Ingenieure, Maschinenbauer, Architecten, etc. H. Dominicus.